are expected to involve macrocycle oxidation and oxidation of Ni^{II} to Ni^{III}, in analogy with Ni(OEP),[59] but further investigation is required in order to make assignments. Unlike M(OEP), the second reductions of M(**5**) (except for M = Mg) are accessible. The first reduction of Mg(**5**) is chemically reversible only at scan speeds in excess of 200 mV/s.

The potentials of H_2(**11**) included in Table V are quite similar to those of H_2(OEC)[31] but differ significantly from those of H_2(**5**). The second oxidation of **11** is totally irreversible. After scanning through this wave, one observes a small unidentified reduction peak at 0.93 V (ECE process) but no reduction of $H_2(\mathbf{11})^{+\cdot}$. Loss of H^+ from the reduced ring β-carbon or from the hydroxyl group of $H_2(\mathbf{11})^{2+}$ are possible explanations of these observations. The former reaction is consistent with the behavior of β-hydrogenated hydroporphyrins.[31]

Conclusions. The results of this investigation of free-base β-oxoporphyrins and metallo-β-oxoporphyrins lead to the following conclusions:

(i) The oxoporphyrin structure type has been confirmed by X-ray structural means.

(ii) The conformations of Ni(**5**) in the solid state deviate from planarity to a lesser extend than those of nickel complexes of hydroporphyrins.

(iii) The carbonyl groups of oxoporphyrins are rather unreactive. Conjugation of the carbonyl to the macrocycle π-system and steric effects may contribute.

(iv) The potentials of the oxidations of oxoporphyrins are similar to those of porphyrins.

(v) The potentials of the reductions become progressively more positive than those of porphyrins and hydroporphyrins as more carbonyl groups are introduced.

(vi) Oxoporphyrins and hydroporphyrins are structurally, electronically, and chemically distinct.

Acknowledgment. We thank the Camille and Henry Dreyfus Foundation (A.M.S.), the Research Corp., the NIH (Grant BRSG S07 RR07044), and the Brandeis Undergraduate Research Program (P.A.G.) for support of this research and Dr. C. K. Chang for providing us with a preprint of ref 17.

Supplementary Material Available: Listings of thermal parameters and nonessential bond lengths (3 pages). Ordering information is given on any current masthead page. According to policy instituted Jan 1, 1986, the tables of calculated and observed structure factors (8 pages) are being retained in the editorial office for a period of 1 year following the appearance of this work in print. Inquiries for copies of these materials should be directed to the Editor.

Contribution from the Department of Chemistry, University of Houston—University Park, Houston, Texas 77004

Ligand-Addition Reactions of Indium(III) Porphyrins. Reactions of (OEP)InX and (TPP)InX with *N*-Methylimidazole and Pyridine

J.-L. Cornillon, J. E. Anderson, and K. M. Kadish*

Received October 21, 1985

The reactions of *N*-methylimidazole (*N*-MeIm) and pyridine with (P)In(X), where P is either the dianion of octaethylporphyrin (OEP) or the dianion of tetraphenylporphyrin (TPP) and X is Cl^-, OAc^-, SO_3Ph^-, or $SO_3CH_3^-$, were monitored by ^1H NMR, electronic absorption spectroscopy, and conductivity measurements. All three methods were self-consistent in demonstrating the stepwise formation of hexacoordinated monomeric In–porphyrin species of the type (P)InX(L) and $[(P)In(L)_2]^+$, where L = pyridine or *N*-MeIm. Equilibrium constants for the ligand-addition reactions of (P)InX and (P)InX(L) were also calculated from the electronic absorption spectra. This is the first time that monomeric, hexacoordinated In(III) porphyrins have been reported.

Introduction

Indium(III) porphyrins of the type (P)InX[1-5] and (P)In(R)[6-9] have been characterized, where P is the dianion of tetraphenylporphyrin (TPP) or octaethylporphyrin (OEP), X is an anionic ligand, and R is one of several different σ-bonded alkyl or aryl groups. Bimetallic indium porphyrins of the form $(P)InM'(L)_n$ have also been reported, where $M'(L)_n$ is an axial ligand of the type $M(CO)_x(\eta^5\text{-}C_5H_5)_y$.[10,11] For the last series of compounds, the indium oxidation state is not known but bimetallic (P)InW-$(CO)_3$Cp has been postulated to contain In(I).[12]

In two recent papers we reported the electrochemistry of ionic[13] and σ-bonded[14] In(III) porphyrins in methylene chloride and benzonitrile. In these nonbonding solvents the In(III) atom is invariably five-coordinate. Six-coordinate In(III) complexes have been characterized in the solid state,[15-17] but such coordination has never been reported for monomeric In(III) porphyrins, which

(1) Buchler, J. W.; Eikelmann, G.; Puppe, L.; Rohbock, K.; Schneehage, H. H.; Weck, D. *Justus Liebigs Ann. Chem.* **1971**, *745*, 135.
(2) Bhatti, M.; Bhatti, W.; Mast, E. *Inorg. Nucl. Chem. Lett.* **1972**, *8*, 133.
(3) Eaton, S. S.; Eaton, G. R. *J. Am. Chem. Soc.* **1975**, *97*, 3660.
(4) Guilard, R.; Cocolios, P.; Fournari, P.; Lecomte, C.; Protas, J. *J. Organomet. Chem.* **1979**, *168*, C49.
(5) Cocolios, P.; Fournari, P.; Guilard, R.; Lecomte, C.; Protas, J.; Boubel, J. C. *J. Chem. Soc., Dalton Trans.* **1980**, 2081.
(6) Cocolios, P.; Guilard, R.; Fournari, P. *J. Organomet. Chem.* **1977**, *129*, C11.
(7) Cocolios, P.; Guilard, R.; Fournari, P. *J. Organomet. Chem.* **1979**, *179*, 311.
(8) Lecomte, C.; Protas, J.; Cocolios, P.; Guilard, R. *Acta Crystallogr., Sect. B: Struct. Crystallogr. Cryst. Chem.* **1980**, *B36*, 2769.
(9) Cocolios, P.; Guilard, R.; Bayeul, D.; Lecomte, C. *Inorg. Chem.* **1985**, *24*, 2058.
(10) Cocolios, P.; Moise, C.; Guilard, R. *J. Organomet. Chem.* **1982**, *228*, C43.
(11) Onaka, S.; Yamashita, M.; Tatematsu, Y.; Kato, Y.; Goto, M.; Ito, T. *Inorg. Chem.* **1985**, *24*, 1070.
(12) Cocolios, P.; Chang, D.; Vittori, O.; Guilard, R.; Moise, C.; Kadish, K. M. *J. Am. Chem. Soc.* **1984**, *106*, 5724.
(13) Kadish, K. M.; Cornillon, J.-L.; Cocolios, P.; Tabard, A.; Guilard, R. *Inorg. Chem.* **1985**, *24*, 3645.
(14) Kadish, K. M.; Boisselier-Cocolios, B.; Cocolios, P.; Guilard, R. *Inorg. Chem.* **1985**, *24*, 2139.
(15) Contreras, J. G.; Einstein, F. W.; Gilbert, M. M.; Tuck, D. G. *Acta Crystallogr., Sect. B: Struct. Crystallogr. Cryst. Chem.* **1977**, *B33*, 1648.
(16) Wignacourt, J. P.; Mairesse, G.; Barbier, P. *Cryst. Struct. Commun.* **1976**, *5*, 293.
(17) Whithow, S. M.; Gabe, E. J. *Acta Crystallogr., Sect. B: Struct. Crystallogr. Cryst. Chem.* **1975**, *B31*, 2534.

0020-1669/86/1325-0991$01.50/0

have only been characterized in solution as five-coordinate species. However, no detailed studies of ligand addition to group 13 porphyrins have ever been reported. Thus, it is of interest to see if six-coordinate indium(III) porphyrins can be produced in solution with the appropriate selection of anion and coordinating ligand. This indeed is the case, as we report in this publication.

We have selected for our initial investigation the reactions of *N*-methylimidazole (*N*-MeIm) and pyridine (py) with (P)InX, where P = OEP or TPP and X = Cl^-, OAc^-, SO_3Ph^-, or $SO_3CH_3^-$. All eight In(III) complexes are ionic, and the structures of (OEP)InOAc and (TPP)$InSO_3CH_3$ have been reported.[5,9] The former compound is bidentate while the latter is polymeric in the solid state. However, only monomeric (P)$InSO_3CH_3$ is present in solutions containing low porphyrin concentrations. Under these conditions, the SO_3R^- group behaves as a weak-binding anion similar to ClO_4^- or PF_6^-.

Experimental Section

Instrumentation. Electronic absorption spectra were recorded with a Tracor Northern 1710 holographic optical spectrometer/multichannel analyzer or an IBM 9430 spectrophotometer. IR spectra were performed on a Perkin-Elmer 1330 spectrometer. Samples were 1% dispersions in CsI pellets. ^1H NMR spectra were performed on a Nicolet FT 300. Samples were typically 3–4 mg/0.5 mL of solvent, CD_2Cl_2, C_6D_6, or pyridine-d_5. An IBM PC/AT computer was used for computation of the stability constants from the raw spectrophotometric data. Solution conductances were determined with a Metrohm A.G. Herisaur Model EA655 cell and a Model 31 YSI conductivity bridge. Measurements were taken at 20.0 ± 0.5 °C.

Chemicals. Electronic absorption spectra were recorded in solutions containing 0.1 M tetrabutylammonium perchlorate (TBAP) (Fluka). This salt was utilized in order to compare data from this study with other spectral data under electrochemical conditions. The TBAP was recrystallized twice from ethanol, dried, and stored under vacuum until use. HPLC grade methylene chloride (CH_2Cl_2) was distilled over CaH_2 prior to use. *N*-Methylimidazole (*N*-MeIm) was vacuum distilled and stored under argon. Pyridine (py) was refluxed over CaH_2 and then distilled over CaH_2 under a nitrogen atmosphere prior to use. CD_2Cl_2, C_6D_6, and pyridine-d_5 were purchased from Aldrich. (TPP)InCl and (OEP)InCl were synthesized according to literature procedures.[2] (P)$In(O_2CCH_3)$ was synthesized by hydrolysis of the In–C σ bond of (P)$InCH_3$[9] with CH_3COOH, and the final isolated complex was recrystallized from a toluene/hexane mixture. The SO_3R^- derivatives were synthesized by a method modified from that previously reported.[5] A typical preparation is described as follows: SO_2 gas was passed through anhydrous CH_2Cl_2 solutions of (P)In(R) at −18 °C for 1 h. The CH_2Cl_2 was removed by vacuum techniques, and toluene was added to the resulting solid. The (P)$InSO_2R$ was oxidized to (P)$InSO_3R$ by addition of O_2 to the toluene solution. The final product was recrystallized from toluene/hexane mixtures. The purity of the acetate and sulfonate derivatives was checked by a comparison of ^1H NMR, IR, and UV–visible spectroscopy results with reported literature values.[5,9]

Methods. Ligand-addition reactions were monitored by changes in the electronic absorption spectra of the complexes, and formation constants for addition of *N*-methylimidazole or pyridine to the In(III) complexes were calculated by the Benesi–Hildebrand method.[18] The overall ligand-addition reactions are given by eq 1 and 2, where L = *N*-MeIm or py.

$$(P)InX + L \overset{K_1}{\rightleftharpoons} (P)InX(L) \quad (1)$$

$$(P)InX(L) + L \overset{K_2}{\rightleftharpoons} [(P)In(L)_2]^+ + X^- \quad (2)$$

Results and Discussion

Formation of (P)$InSO_3R$(*N*-MeIm) and $[(P)In(N\text{-MeIm})_2]^+$. The reactions of *N*-MeIm with (P)$InSO_3R$ were monitored by ^1H NMR, conductivity, and electronic absorption spectroscopy. Studies of the four metalloporphyrins by the three techniques gave internally self-consistent results that are in agreement with the successive formation of mono and the bis *N*-MeIm adducts to (P)$InSO_3R$.

The formation of (P)$InSO_3Ph$(*N*-MeIm) rather than $[(P)In(N\text{-MeIm})]^+$ is evident from the ^1H NMR spectra, which were obtained during a titration of (P)$InSO_3Ph$ with *N*-MeIm. These results are illustrated in Figure 1, which is the ^1H NMR spectra of 10^{-3} M (TPP)$InSO_3Ph$ in CD_2Cl_2 with increasing amounts of *N*-MeIm. In the absence of coordinating ligand, the ^1H NMR spectrum in Figure 1a is obtained. This spectrum is similar to the reported ^1H NMR spectrum of (TPP)$InSO_3Ph$ in $CDCl_3$.[5] It is characterized by resonances of the porphyrin protons at 9.12, 8.22, and 7.81 ppm and by resonances for the bound SO_3Ph^- group at 5.25, 6.74, and 7.04 ppm. These latter signals have been assigned as the ortho, meta, and para proton resonances of SO_3Ph^-, respectively.

Figure 1. ^1H NMR spectra of (TPP)$InSO_3Ph$, 10^{-3} M in CD_2Cl_2, containing the following amounts of *N*-MeIm: (a) none; (b) 1 equiv; (c) 2 equiv; (d) 6 equiv. ● indicates the *N*-MeIm protons, and ▼ is the solvent signal. The insert shows the *N*-MeIm labeling.

Upon addition of 1 equiv of *N*-MeIm, no changes in chemical shifts are observed for either the porphyrin or the SO_3Ph^- proton resonances. Changes are, however, observed in the resonances of the *N*-MeIm protons. In CD_2Cl_2, uncomplexed *N*-MeIm shows four peaks at 7.36 (H_c), 6.95, 6.86 (H_a, H_b), and 3.62 ppm (CH_3). (See insert in Figure 1a for proton labeling.) The *N*-MeIm proton resonances are shifted upfield in the presence of (TPP)$InSO_3R$ by about 1 ppm to 2.42 ppm for the CH_3 signals and by about 4–5 ppm to 2.15 and 2.76 ppm for the H_a and H_b signals as compared to those for free, uncomplexed *N*-MeIm. The absence of any variation in the SO_3Ph^- signal and the dramatic upfield shift of the resonances assigned to the *N*-MeIm protons clearly show that both SO_3Ph^- and *N*-MeIm are bound to the In(III) complex after the addition of 1 equiv of *N*-MeIm. Furthermore, hexacoordination of In(III) results in an inequivalence of the porphyrin ortho phenyl protons. Thus, only one broad peak is observed at 8.22 ppm in the absence of *N*-MeIm (Figure 1a) but two sharp peaks at 8.21 and 8.19 ppm are observed in solutions containing 1 equiv of *N*-MeIm (Figure 1b).

Addition of a second equivalent of *N*-MeIm to (TPP)In(SO_3Ph)(*N*-MeIm) (Figure 1c) leads to the complete disappearance of the SO_3Ph^- ortho proton signal and a shift of about 0.3 ppm to 6.98 and 7.27 ppm for the meta and para protons of the SO_3Ph^- group, respectively. The signal from the ortho protons of the SO_3Ph^- group is more sensitive to changes in coordination with the indium atom. The complete disappearance of the signal is interpreted as resulting from a fast ligand exchange between free *N*-MeIm and the SO_3Ph^- group on (TPP)In(SO_3Ph)(*N*-MeIm). An exchange in these cases is also observed at higher concentrations of *N*-MeIm, but the exchange is only between bound and unbound *N*-MeIm ligands. The signal arising from *N*-MeIm (H_a, H_b) begins to broaden and to move downfield as

(18) Benesi, H. A.; Hildebrand, J. H. *J. Am. Chem. Soc.* **1949**, *71*, 2703.

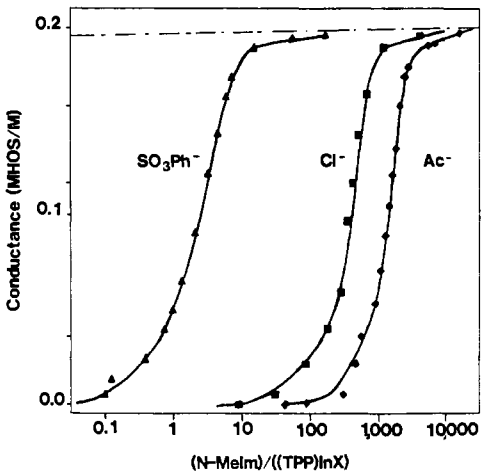

Figure 2. Variation of the equivalent conductance of a 10^{-3} M (TPP)InX solution in CH_2Cl_2 as a function of *N*-MeIm/(TPP)InX. The dashed line represents the equivalent conductance of a 1×10^{-3} M solution of TBAP.

the concentration of *N*-MeIm is increased. This is shown in Figure 1c,d. A similar exchange between free and complexed ligand has been observed by Kadish and Goff[19] for the addition of pyridine to $[(TPP)Fe]_2N$. Similar NMR results were obtained with $(OEP)In(SO_3Ph)$ and *N*-MeIm.

The loss of the bound anionic ligand from In(III) is shown by conductivity measurements of (P)InX in solutions of different CH_2Cl_2/*N*-MeIm ratios. Figure 2 shows the variation of the conductance for 10^{-3} M solutions of (TPP)InX in CH_2Cl_2 containing increasing *N*-MeIm/(TPP)InX ratios. In the absence of coordinating ligand the conductivity is zero. However, as *N*-MeIm is added to solutions of CH_2Cl_2, the conductivities of all three porphyrins increase until a limiting value of about 0.20 Ω^{-1}/M is obtained in each case. The binding strength between the anionic ligand and the In(III) atom increases in the order $SO_3Ph^- < Cl^- < CH_3CO_2^-$, and this agrees with the results shown in Figure 2. The weakest interaction is between $[(P)In]^+$ and SO_3Ph^-, and for $(P)InSO_3Ph$, the addition of *N*-MeIm occurs at very low ligand concentrations. The addition of 1 equiv leads to some dissociation of SO_3Ph^-, but at least 4 equiv of *N*-MeIm are needed for complete dissociation to occur. A similar anion dissociation occurs for (TPP)InCl and (TPP)InOAc, but for these complexes, an 800–1200-fold excess of *N*-MeIm is needed. Thus, both ^1H NMR and conductivity measurements are consistent with the stepwise ligand addition reaction shown in eq 1 and 2.

Formation of $[(P)InSO_3R(py)]$ and $[(P)In(py)_2]^+$. The ^1H NMR spectra of $(TPP)In(SO_3Ph)$ in CD_2Cl_2 with different concentrations of pyridine are shown in Figure 3. Figure 3a shows the ^1H NMR spectrum in the absence of pyridine while Figure 3b is the spectrum obtained after addition of 1 equiv of pyridine. Similar to the case of *N*-MeIm, few changes were observed for the signals from $(TPP)In(SO_3Ph)$, but large changes were observed for the pyridine signals. Uncomplexed pyridine in CD_2Cl_2 has signals at 8.55, 7.51, and 7.19 ppm assigned to the ortho, para, and meta protons, respectively. The pyridine ortho proton resonance in Figure 3b is shifted by almost 3 ppm from the uncomplexed signal to 5.74 ppm. Clearly, this indicates formation of a six-coordinate species. Upon further addition of pyridine, the same basic effects are observed as the *N*-MeIm case. The most dramatic of the changes is the downfield shift of the pyridine ortho proton signal as the concentration of pyridine is increased. Again, this is due to a fast ligand exchange between the complexed and uncomplexed pyridine ligands. This is shown in Figure 3c,d.

The ^1H NMR spectrum of $(OEP)InSO_3CH_3$ in neat pyridine-d_5 clearly shows the formation of $[(OEP)In(py)_2]^+SO_3CH_3^-$ in solution. This is demonstrated in Figure 4, which is the ^1H NMR

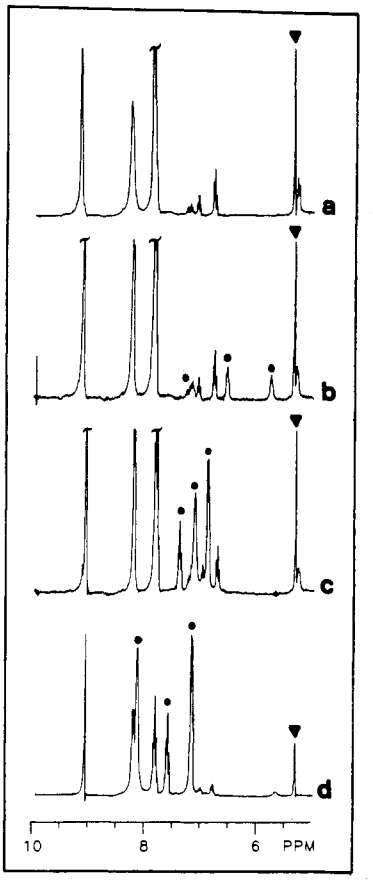

Figure 3. ^1H NMR spectra of $(TPP)InSO_3Ph$, 10^{-3} M in CD_2Cl_2, containing the following amounts of py: (a) none; (b) 1 equiv; (c) 5 equiv; (d) 18 equiv. ● indicates the py protons, and ▼ is the solvent signal.

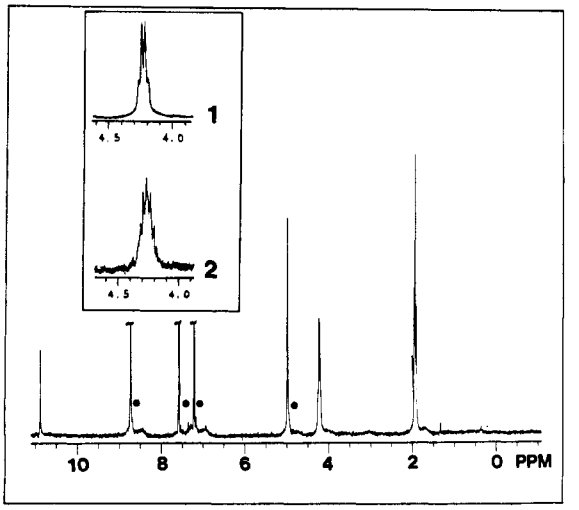

Figure 4. ^1H NMR spectrum of $(OEP)InSO_3CH_3$ in pyridine-d_5. The insert shows the methylenic proton signal of $(OEP)InSO_3CH_3$ in (1) pyridine-d_5 and (2) CD_2Cl_2. Marked peaks are signals arising from the solvents.

spectrum of $(OEP)InSO_3CH_3$ in pyridine-d_5. The ^1H NMR of $(OEP)In(SO_3CH_3)$ in CD_2Cl_2 is essentially the same as that reported for $CDCl_3$[5] and is typical of a metalloporphyrin species.[20] The signals at 10.35, 4.18, and 1.93 ppm are due to the octaethylporphyrin proton resonances. The bound $SO_3CH_3^-$ resonance is at −0.36 ppm; nonligated $SO_3CH_3^-$ is observed at 2 ppm. One of the insets in Figure 4 shows the methylenic proton signal of $(OEP)In(SO_3CH_3)$ in neat pyridine-d_5. The main difference

(19) Kadish, K. M.; Rhodes, R. K.; Bottomley, L. A.; Goff, H. M. *Inorg. Chem.* **1981**, *20*, 3195.

(20) Janson, T. R.; Katz, J. J. In "The Porphyrins"; Dolphin, D., Ed.; Academic Press: New York, 1979; Vol. 4.

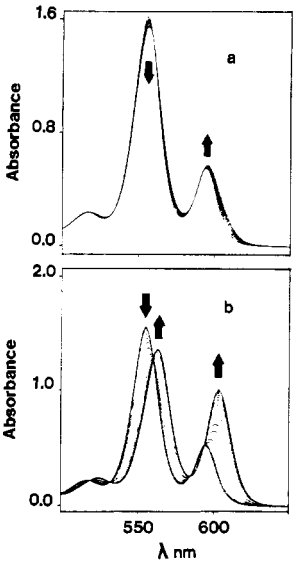

Figure 5. UV–visible spectra taken during the titration of 5×10^{-5} M (TPP)$InSO_3Ph$ by *N*-MeIm in CH_2Cl_2, 0.1 M TBAP: (a) first ligand addition up to 1.1 equiv of *N*-MeIm added; (b) second ligand addition from 2 to 400 equiv of *N*-MeIm added.

between the spectrum in CD_2Cl_2 and that in pyridine-d_5 is the downfield shift of the $SO_3CH_3^-$ protons from −0.36 ppm to 1.99 ppm. Clearly, the In–SO_3CH_3 bond has been broken and the signal due to the $SO_3CH_3^-$ protons is due to uncomplexed $SO_3CH_3^-$.

Busby and Dolphin[21] have shown that the methylenic protons of the metal–octaethylporphyrin system are anisochronous if the metal does not possess planar symmetry with respect to the porphyrin plane. The signal arising from the methylenic protons of 5×10^{-4} M (OEP)$InSO_3CH_3$ in CH_2Cl_2 exhibits at least eight peaks resulting from the inequivalence of the two methylenic protons, but in neat pyridine, a well-defined quadruplet is obtained showing the equivalence of the two methylenic protons. (See inserts 1 and 2 of Figure 4.) This implies an equivalence of the porphyrin face and thus a hexacoordination of the In(III) atom. The formulation of the complex as $[(OEP)In(py)_2]^+$ follows from the data.

Interaction of (P)InOAc and (P)InCl with Pyridine. No evidence was observed for the binding of pyridine by (P)InOAc or (P)InCl in either CH_2Cl_2/py mixtures or in neat pyridine. The conductivity of these complexes is close to zero in both CH_2Cl_2 and in neat pyridine, as well as in all solutions containing different py/CH_2Cl_2 ratios. This conductivity measurement rules out the dissociation of X^- from (P)InX and is consistent with the formation of either (P)InX(py) or (P)InX in neat pyridine. No significant differences are observed between the electronic absorption spectra of a given TPP or OEP complex in pyridine, py/CH_2Cl_2 mixtures, or CH_2Cl_2. Only small changes are observed on formation of (P)InX(*N*-MeIm) so that this is not a reliable criterion for ruling against (P)InX(py) formation. However, the ^1H NMR spectra of (TPP)InCl, (TPP)InOAc, (OEP)InCl, and (OEP)InOAc are virtually identical in CH_2Cl_2 and in pyridine. Also, titration of (OEP)InCl in CD_2Cl_2 with pyridine leads to no change in the (OEP)InCl signals and less than 0.02 ppm variation for the signals of the pyridine protons compared to signals of the free pyridine. All of the results are self-consistent and suggest that there is, at best, a very weak interaction between (P)InOAc or (P)InCl and pyridine. This is not the case for (P)$InSO_3R$, which may form both mono- and bis(pyridine) adducts depending on the concentration of pyridine.

Monitoring of Ligand Addition by Electronic Absorption Spectra and Calculation of Formation Constants. The titration of 5.0×10^{-5} M (TPP)$InSO_3Ph$ with *N*-MeIm leads first to (TPP)$InSO_3Ph$(*N*-MeIm) and then to the final species characterized as $[(TPP)In(N\text{-MeIm})_2]^+$. The electronic absorption spectrum of (TPP)$InSO_3Ph$ is shown in Figure 5 and is typical of a "normal" metalloporphyrin spectrum.[22] The complex has three absorption bands, which are located at 426, 555, and 694 nm. Upon addition of less than 1 equiv of *N*-MeIm, the band at 558 nm slightly decreases in intensity while the band at 697 nm shifts toward 699 nm. This is shown in Figure 5a. Larger additions of *N*-MeIm to the above solution lead to a red shift of the entire spectrum, and the final spectrum is characterized by bands at 561 and 604 nm. This spectrum is shown in Figure 5b. Clear isosbestic points are obtained between 2 equiv of *N*-MeIm and the final *N*-MeIm concentration, indicating that under these conditions only two species are present in solution.

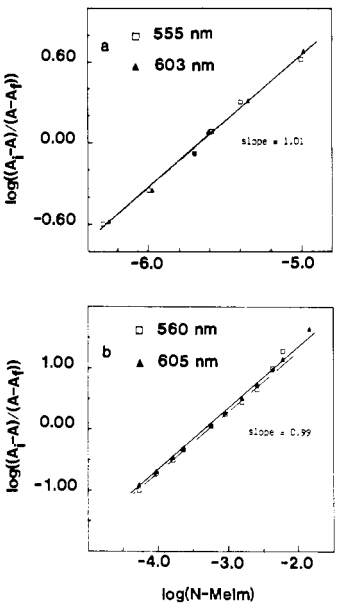

Figure 6. Analysis of spectral data for the titration of (TPP)$InSO_3Ph$ with *N*-MeIm in CH_2Cl_2, 0.1 M TBAP: (a) first ligand addition; (b) second ligand addition. Data taken from Figure 5.

Table I. Stability Constants for Addition of *N*-Methylimidazole and Pyridine to (P)InX in CH_2Cl_2

porphyrin macrocycle	anion, X	*N*-MeIm log K_1[a]	*N*-MeIm log K_2[b]	py log K_1	py log K_2[b]
TPP	SO_3Ph^-	5.7	3.3	*d*	1.9
	$SO_3CH_3^-$	5.5	3.3	*d*	2.1
	Cl^-	*e*	1.0	NR[c]	NR
	OAc^-	*e*	0.8	NR[c]	NR
OEP	SO_3Ph^-	5.2	3.0	*d*	1.7
	$SO_3CH_3^-$	5.3	3.0	*d*	1.6
	Cl^-	*e*	1.2	NR[c]	NR
	OAc^-	*e*	0.7	NR[c]	NR

[a] Reaction 1; log K ±0.4. [b] Reaction 2; log K ±0.2. [c] See text; NR = no reaction. [d] Greater than 4.5 from ^1H NMR data. [e] Greater than 3 from ^1H NMR data.

Analysis of the spectral changes in Figure 5 was carried out as a function of ligand concentration and leads to plots of the type shown in Figure 6. Two separate ligand addition steps are observed. Analysis of the two sets of spectral changes give straight-line plots with a slope of 1.0, and from this data, values of log K_1 = 5.7 ± 0.4 and log K_2 = 3.3 ± 0.2 were obtained.

Results for (TPP)$InSO_3Ph$, (OEP)$InSO_3Ph$, and (OEP)-$InSO_3CH_3$ were similar to those described above for (TPP)-$InSO_3Ph$. The addition of 1 equiv of *N*-MeIm to (P)$InSO_3R$ showed the initial formation of (P)$InSO_3R$(*N*-MeIm) while addition of 1–10 equiv of *N*-MeIm led to $[(P)In(N\text{-MeIm})_2]^+$ as shown in eq 2. The stability constants for reactions 1 and 2 were

(21) Busby, C. A.; Dolphin, D. *J. Magn. Reson.* **1976**, *23*, 211.

(22) Gouterman, M. In "The Porphyrins"; Dolphin, D., Ed.; Academic Press: New York, 1979; Vol. 3.

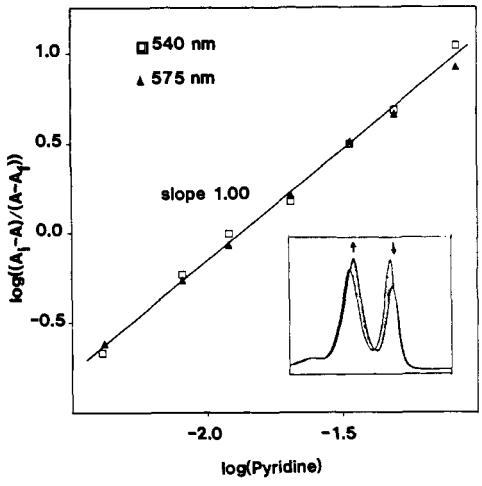

Figure 7. Analysis of spectral data for the titration of 5×10^{-5} M $(OEP)InSO_3CH_3$ with pyridine in CH_2Cl_2, 0.1 M TBAP. The insert represents the visible spectral variations during the titration.

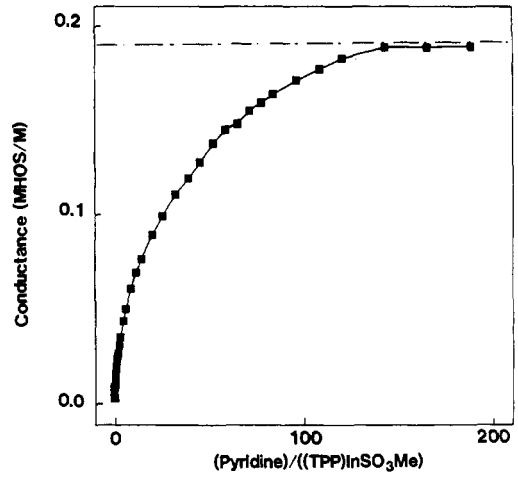

Figure 8. Plot of equivalent conductance for the titration of 5×10^{-4} M $(TPP)InSO_3CH_3$ with pyridine in CH_2Cl_2. The dashed line represents the equivalent conductance of a 5×10^{-4} M solution of TBAP.

independent of the R group on SO_3R^- and were slightly smaller for the OEP complexes than for the TPP complexes. These values are listed in Table I.

Both mono- and bis(ligand) adducts form when *N*-MeIm is added to CH_2Cl_2 solutions of (P)InOAc and (P)InCl, but formation constants for the first ligand addition could not be calculated due to the fact that only small differences exist between the absorption spectra of (P)InX and (P)InX(*N*-MeIm). However, changes in the UV–visible spectra are large during the second ligand addition to (P)InX(*N*-MeIm) and values of log K_2 between 0.7 and 1.2 were calculated. These values are listed in Table I. Evidence that the calculated values correspond to those of reaction 2 and not to those of reaction 1 comes from the fact that the final electronic absorption spectra are identical for all of the (P)InX complexes of a given OEP or TPP series in *N*-MeIm solutions as well as the fact that the conductivity data (Figure 2) clearly show dissociation of the anionic ligand on (P)InX at high *N*-MeIm concentrations.

As discussed above, the addition of pyridine to (P)InOAc or (P)InCl in CH_2Cl_2 produced no detectable spectroscopic changes, nor was there any difference in the spectra between neat CH_2Cl_2 and neat pyridine. On the other hand, the addition of pyridine to complexes of $(P)InSO_3R$ in CH_2Cl_2 did lead to well-defined changes in the electronic absorption and the ^1H NMR spectra and from the former changes the values of formation constants for the binding of pyridine could be calculated.

An example of the spectral changes associated with the formation of $[(OEP)In(py)_2]^+$ from $(OEP)InSO_3Ph(py)$ in CH_2Cl_2/py mixtures and an analysis of the spectral data are shown in Figure 7. As seen in the insert, there is a red shift of the entire $(OEP)InSO_3Ph$ spectrum upon addition of pyridine. The new species has a Soret band at 411 nm and two visible bands at 540 and 578 nm. Again, the large changes in the UV–visible spectra are due to the formation of $[(P)In(py)_2]^+$. Analysis of the spectral changes as a function of pyridine concentration leads to a straight plot with a slope of 1.0 (see Figure 7), from which log $K_2 = 1.6 \pm 0.2$ can be calculated. Similar results were obtained for the other $(P)InSO_3R$ complexes, and values of log K_2 are listed in Table I for comparison with the data for addition of *N*-MeIm to (P)InX.

Titrations of $(P)InSO_3R$ with pyridine were also monitored by conductivity, and a plot of conductance vs. the $(py)/(P)InSO_3CH_3$ ratio in CH_2Cl_2/py mixtures is shown in Figure 8. The final conductance is almost identical with the conductance obtained for the same concentration of a 1/1 electrolyte (TBAP or TBA-(PF_6)) in the same CH_2Cl_2/py mixture. In addition, the final equivalent conductance is within experimental error of that shown for $[(P)In(N\text{-MeIm})_2]^+$ in Figure 2.

In summary, we have shown that both mono- and bis(ligand) adducts may be formed from indium(III) porphyrins containing a weak-field anionic ligand. These results are of interest in evaluating the reactions of In(III) porphyrins with diatomic molecules, where the formation of a six-coordinate complex in a low (In(II)) oxidation state has been proposed.[9] In addition, the presence of *N*-MeIm or pyridine that is axially bound to the In(III) complex will significantly alter the redox chemistry of the metalloporphyrin. This will be discussed in a future publication.

Acknowledgment. The support of the National Science Foundation (Grant CHE-8215507) is gratefully acknowledged. We acknowledge several fruitful discussions with Professor Roger Guilard of the University of Dijon. Ed Ezell is also acknowledged for his help with obtaining the NMR spectra.

Registry No. $(TPP)InSO_3Ph$, 70619-92-0; $(TPP)InSO_3CH_3$, 70619-88-4; (TPP)InCl, 63128-70-1; (TPP)InOAc, 96150-61-7; $(OEP)InSO_3Ph$, 70619-98-6; $(OEP)InSO_3CH_3$, 70619-94-2; (OEP)InCl, 32125-07-8; (OEP)InOAc, 96150-60-6; *N*-MeIm, 616-47-7; pyridine, 110-86-1.